

## Epitaxial growth of germanium on silicon using a Gd<sub>2</sub>O<sub>3</sub>/Si (111) crystalline template

G. Niu, L. Largeau, G. Saint-Girons, B. Vilquin, J. Cheng et al.

Citation: *J. Vac. Sci. Technol. A* **28**, 1187 (2010); doi: 10.1116/1.3478301

View online: <http://dx.doi.org/10.1116/1.3478301>

View Table of Contents: <http://avspublications.org/resource/1/JVTAD6/v28/i5>

Published by the AVS: Science & Technology of Materials, Interfaces, and Processing

---

### Additional information on *J. Vac. Sci. Technol. A*

Journal Homepage: <http://avspublications.org/jvsta>

Journal Information: [http://avspublications.org/jvsta/about/about\\_the\\_journal](http://avspublications.org/jvsta/about/about_the_journal)

Top downloads: [http://avspublications.org/jvsta/top\\_20\\_most\\_downloaded](http://avspublications.org/jvsta/top_20_most_downloaded)

Information for Authors: [http://avspublications.org/jvsta/authors/information\\_for\\_contributors](http://avspublications.org/jvsta/authors/information_for_contributors)

## ADVERTISEMENT



 Advance your technology or engineering career using the **AVS Career Center**, with **hundreds of exciting jobs** listed each month!

<http://careers.avs.org>



# Epitaxial growth of germanium on silicon using a $\text{Gd}_2\text{O}_3/\text{Si}$ (111) crystalline template

G. Niu<sup>a)</sup>

*Ecole Centrale de Lyon, INL/UMR CNRS-5512, 36 Avenue Guy de Collongue, 69134 Ecully, France*

L. Largeau

*LPN-UPR20/CNRS, Route de Nozay, 91460 Marcoussis, France*

G. Saint-Girons, B. Vilquin, and J. Cheng

*Ecole Centrale de Lyon, INL/UMR CNRS-5512, 36 Avenue Guy de Collongue, 69134 Ecully, France*

O. Mauguin

*LPN-UPR20/CNRS, Route de Nozay, 91460 Marcoussis, France*

G. Hollinger

*Ecole Centrale de Lyon, INL/UMR CNRS-5512, 36 Avenue Guy de Collongue, 69134 Ecully, France*

(Received 12 May 2010; accepted 20 July 2010; published 3 September 2010)

This work presents a study of the epitaxial growth of Ge on Si (111) using a  $\text{Gd}_2\text{O}_3$  crystalline template. A smooth two-dimensional Ge layers is obtained from the coalescence of initially three-dimensional Ge islands grown in the Volmer–Weber mode. Ge takes its bulk lattice parameter at the very early stages of its growth. A detailed x-ray pole figure analysis reveals that the epitaxial relationship between the layers and the Si substrate is  $[1-10]\text{Ge}(111)\parallel[-110]\text{Gd}_2\text{O}_3(111)\parallel[1-10]\text{Si}(111)$  and that microtwins are formed in the Ge layer. © 2010 American Vacuum Society. [DOI: 10.1116/1.3478301]

## I. INTRODUCTION

The integration of a high quality germanium epilayers on Si has motivated numerous researches in the recent years. Due to its high hole mobility, Ge appears as an interesting channel material alternative to Si for high-frequency metal oxide semiconductor field-effect transistor (*p*-MOSFETs). Ge/Si crystalline templates could also be used as templates for the integration of III-V based heterostructures on standard industrial Si wafer, thanks to the negligible lattice mismatch between Ge and GaAs ( $\sim 0.12\%$ ). Fabricating such heterostructures could allow combining high-performance micro- and optoelectronic functionalities on the same silicon base wafer. The direct epitaxy of Ge on Si is challenging: the lattice mismatch between these two materials is about 4.1%, so that threading dislocations are generated in the growing material once the deposited thickness exceeds a critical thickness<sup>1</sup> of a few monolayers. Many strategies have been developed to overcome this difficulty, and several recent studies have demonstrated the opportunity of using crystalline oxides/Si templates such as  $\text{SrHfO}_3/\text{Si}$  (001),<sup>2</sup>  $\text{PrO}_2/\text{Si}$  (111),<sup>3</sup>  $\text{SrTiO}_3/\text{Si}$  (001),<sup>4-6</sup> and  $\text{Gd}_2\text{O}_3/\text{Si}$  (111) (Ref. 7) for the integration of Ge or III-V materials on silicon. Due to the strong crystallographic and chemical heterogeneity between III-V or IV-IV semiconductors and oxides, the elevated lattice mismatch between these materials is fully accommodated by a network of dislocations, confined at the heterointerface, and formed at the very early stages of the growth. As a consequence, the semiconductor grows with its bulk lattice

parameter on the oxide surface and does not contain any threading defect related to any plastic relaxation mechanism, as explained in detail in one of our earlier studies.<sup>8</sup> Schroeder *et al.* extensively studied the  $\text{Ge}/\text{Pr}_2\text{O}_3/\text{Si}$  (111) system. They demonstrated that  $\text{Pr}_2\text{O}_3/\text{Si}$  (111) templates could be used for the integration of single crystal two-dimensional Ge layers on Si<sup>3</sup>. Simple geometric considerations indicate that two Ge domains should be formed on the  $\text{Pr}_2\text{O}_3$  (111) surface. Schroeder *et al.* showed that electrostatic effects at the heterointerface select one of these two domains, leading to a single domain Ge growth.<sup>9</sup> Furthermore, this group has recently evidenced that microtwins were formed in Ge epilayers grown on  $\text{Pr}_2\text{O}_3/\text{Si}$  (111) templates, due to the fact that these layers result from the coalescence of initially three-dimensional Ge islands.<sup>10</sup>

In this work, we show that  $\text{Gd}_2\text{O}_3/\text{Si}$  (111) epilayers can also be used as templates for the integration of Ge on Si.  $\text{Gd}_2\text{O}_3$  has the same bixbyite crystal structure as  $\text{Pr}_2\text{O}_3$  but presents some interesting features: Gd is a single valence metal ion (+3), so that  $\text{Gd}_2\text{O}_3$  is the single stable Gd oxide, while both  $\text{Pr}_2\text{O}_3$  and  $\text{PrO}_2$  oxides can be formed. Moreover,  $\text{Gd}_2\text{O}_3$  is more stable in air than  $\text{Pr}_2\text{O}_3$ . In the end,  $\text{Gd}_2\text{O}_3/\text{Si}$  (111) templates present a high monocrystalline quality, as recently demonstrated in Ref. 11. Based on the detailed reflection high energy electron diffraction (RHEED) and x-ray diffraction (XRD) analyses, we show (i) that Ge takes its bulk lattice parameter as soon as the growth begins, thus obeying the specific accommodation mode described in Ref. 8; (ii) that Ge contains microtwins, the proportion of twinned material being precisely determined.

<sup>a)</sup>Electronic mail: gang.niu@ec-lyon.fr

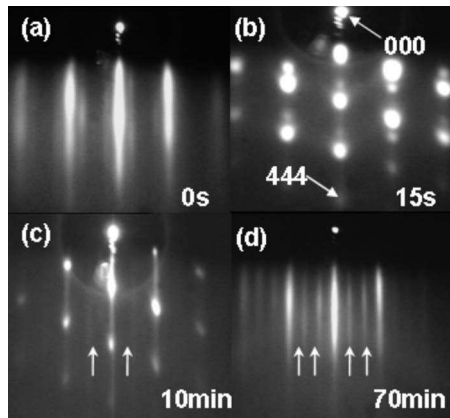


FIG. 1. Evolution of the RHEED patterns as a function of Ge thickness. The arrows in (c) and (d) highlight the Ge surface reconstructions.

## II. EXPERIMENT

The sample considered in the following was grown on a nominally (111)-oriented silicon substrate. Before growth, the Si substrate was cleaned using a  $\text{HF-NH}_4\text{F}$  solution. The H-terminated substrate was then introduced in the solid-source molecular beam epitaxy chamber (RIBER EVA 32 reactor), and a 6 nm thick (111)-oriented  $\text{Gd}_2\text{O}_3$  layer was grown (at 700 °C and under a partial  $\text{O}_2$  pressure of  $10^{-6}$  Torr, using an electron beam evaporated single crystal  $\text{Gd}_2\text{O}_3$  target, as extensively described in Ref. 11). A 280 nm Ge layer was then grown (using a standard Knudsen cell) on this  $\text{Gd}_2\text{O}_3/\text{Si}$  (111) template, at 400 °C and at a growth rate of 4  $\text{nm min}^{-1}$ . The sample was characterized *in situ* by RHEED (30 kV e-beam gun) and *ex situ* by XRD (pole figure and rocking curve measurements) using a Panalytical X'Pert Pro diffractometer.

## III. RESULTS AND DISCUSSION

### A. Accommodation and growth mode

Figure 1 shows the evolution of the RHEED pattern (recorded along one of the  $\text{Gd}_2\text{O}_3$   $\langle 110 \rangle$  azimuths) during Ge growth. Before Ge growth starts, the  $\text{Gd}_2\text{O}_3$  surface [Fig. 1(a)] presents well-defined streaky lines and a clear  $\times 4$  reconstruction, indicating the good crystal and surface quality of the oxide template. Once Ge growth begins, the pattern turns spotty [Fig. 1(b)] indicating an initial three-dimensional growth in the Volmer–Weber mode. At this stage of the growth, the RHEED pattern is very similar to that observed in Ref. 3 during the growth of Ge on  $\text{PrO}_2/\text{Si}$  (111) templates, or even to that observed during the growth of InP on  $\text{Gd}_2\text{O}_3/\text{Si}$  (111) templates.<sup>7</sup> As explained in Ref. 3, this pattern results from the superimposition of the (111)-oriented Ge Bragg peaks and of the diffraction of uncovered oxide regions. After the deposition of 40 nm of Ge, the RHEED pattern starts exhibiting diffraction lines, indicating that the initially formed Ge islands coalesce to form a two-dimensional layer. In Fig. 1(c), a clear  $\times 2$  reconstruction of the Ge surface can be observed. At the end of the growth [Fig. 1(d)], the RHEED pattern presents bright streaky lines

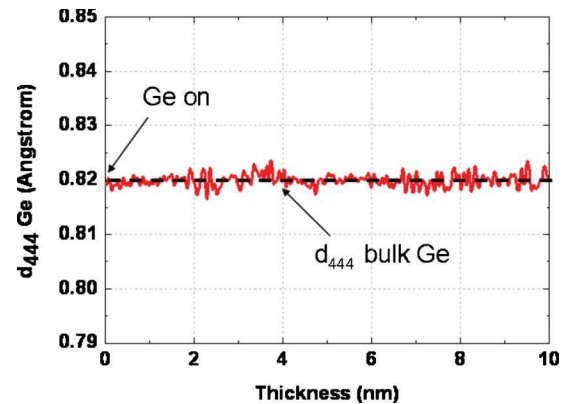
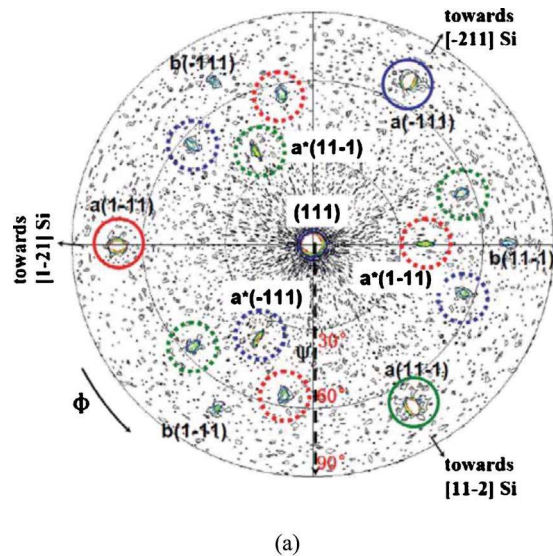


FIG. 2. (Color online) Evolution of the 444 interatomic distance during the early stages of the Ge growth.  $d_{444}$  remains constant ( $\sim 0.82$  Å) and equals to its value of bulk Ge.

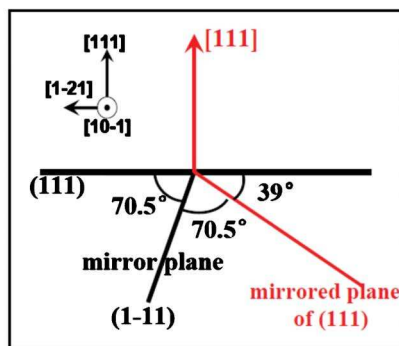
resulting from the diffraction of a flat and well crystallized Ge epilayer. The Ge surface presents a  $(3 \times 3)$  reconstruction, already observed for Ge(111) surfaces, possibly with the impurity of carbon or gadolinium.<sup>12</sup> The evolution of the out-of-plane Ge 444 interatomic distance during the early stages of the growth was measured by recording the evolution of distance between the 000 transmitted spot and the 444 Ge reflection spot on the RHEED pattern [as indicated in Fig. 1(b)]. The result is displayed in Fig. 2. The RHEED camera length was calibrated assuming that the Si substrate presents the bulk Si lattice parameter. The Ge 444 interatomic distance remains constant and equals to its value in bulk Ge ( $\approx 0.82$  Å) during Ge growth. In particular, Ge takes its bulk lattice parameter as soon as it can be measured by RHEED. This behavior has already been observed for several semiconductor/oxide systems.<sup>7,8</sup> For standard mismatched IV-IV or III-V systems, the growing material takes the in-plane lattice parameter of the substrate at the early stages of the growth and undergoes a plastic relaxation process during which it progressively recovers its bulk lattice parameter at the expense of the formation of threading dislocations. In contrast here, Ge takes its bulk lattice parameter as soon as growth begins. The lattice mismatch between Ge and  $\text{Gd}_2\text{O}_3$  is fully accommodated by forming interface dislocations confined at the heterointerface, as described in Ref. 7 for the InP/ $\text{Gd}_2\text{O}_3$  system or in Ref. 8 for the InP/ $\text{SrTiO}_3$  system.

### B. Epitaxial relationship and evidence for twin formation in the Ge layer

X-ray pole figures were recorded on the sample. For that purpose, the x-ray incident beam was point focused onto a 10  $\text{mm}^2$  area using a polycapillary lens and crossed slits. A Ge 111 pole figure is shown in Fig. 3(a). On this figure, the radial scale corresponds to the polar angle ( $\psi$ ), while the azimuthal incidence ( $\phi$ ) varies along the perimeter. The  $2\theta$  angle was fixed at  $27.28^\circ$ , which corresponds to the Ge 111 Bragg angle. Thus, all the visible reflections on the pole figure correspond to the diffraction of planes with interplanar distances close to the Ge  $\{111\}$  planes. The coordinates of



(a)



(b)

FIG. 3. (Color online) (a) X-ray pole figure recorded near the 111 Si reflections on the sample of  $\text{Ge}/\text{Gd}_2\text{O}_3/\text{Si}$  (111). (b) Sketch of the twinning sequence for one of the  $\text{Ge}$   $\{111\}$  plane family.

these reflections allow orientating the different  $\text{Ge}$  variants with respect to each other in the real space. Additionally, for each reflection in the pole figure of Fig. 3(a), defined by its polar and azimuthal angles, rocking curves were recorded in order to scan the reciprocal space, measure the lattice parameters, and thus detect the different layers of the heterostructure, namely, the  $\text{Si}$  substrate, the  $\text{Gd}_2\text{O}_3$  template, and the  $\text{Ge}$  layer and determine their relative orientations. Some of these rocking curves are plotted in Fig. 4. Using these rocking curves, the pole figure of Fig. 3(a) has been fully indexed. The spot in the center labeled (111) (symmetric conditions) indicates that  $\text{Ge}$  is (111)-oriented (same out-of-plane orientation as the  $\text{Si}$  substrate). The threefold symmetric reflections located at  $\psi=70^\circ$  and  $\phi=60^\circ, 180^\circ$ , and  $300^\circ$  and labeled  $a(-111)$ ,  $a(1-11)$ , and  $a(11-1)$  correspond to the main variant of the  $\text{Ge}$  crystal, designated as variant  $a$ . The other reflections in the pole figure correspond to the presence of twinned  $\text{Ge}$  variants in the layer. The set of low-intensity threefold symmetric reflections at  $\psi=70^\circ$  and  $\phi=0^\circ, 120^\circ$ , and  $240^\circ$  [labeled  $b(-111)$ ,  $b(1-11)$ , and  $b(11-1)$ ] indicate the presence of a second  $\text{Ge}$  variant in the layer (labeled variant  $b$ ), twisted of  $60^\circ$  around the  $\text{Ge}$  (111) ver-

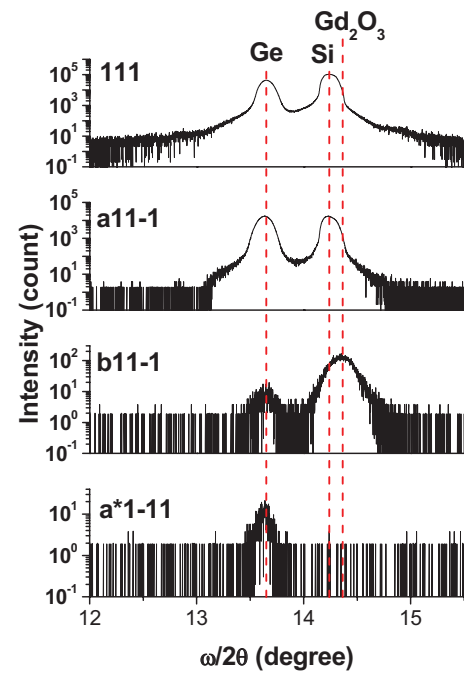


FIG. 4. (Color online) Rocking curves corresponding to the spots in the x-ray pole figure in Fig. 3(a).

tical direction with respect to variant  $a$ . This variant  $b$  corresponds to the presence of the twinning with respect to the  $\text{Ge}(111)$  surface. The mirror planes of these microtwins are the  $(-111)$ ,  $(1-11)$ , and  $(11-1)$   $\text{Ge}$  inclined planes, respectively. Simple geometric considerations allow concluding that the other reflections in the pole figure result from the presence of twins in the  $\text{Ge}$  layer. The reflections marked by red, green, and blue dotted circles correspond to the twinning of the  $\text{Ge}(111)$  surface plane relatively to the  $\text{Ge}(1-11)$ ,  $(11-1)$ , and  $(-111)$  inclined planes, respectively. This twinning sequence is sketched in Fig. 3(b) for the  $\text{Ge}(1-11)$  plane. On this figure, the trace of the (111) and (1-11)  $\text{Ge}$  planes are plotted in the (10-1)  $\text{Ge}$  plane. In this plane, the symmetric of the  $\text{Ge}(111)$  plane with respect to the trace of the  $\text{Ge}(1-11)$  planes (mirror plane) is labeled as mirrored plane of (111). It forms an angle of  $39^\circ$  with respect to the  $\text{Ge}(111)$  planes. These planes, corresponding to the twin of the  $\text{Ge}(111)$  planes with respect to the  $\text{Ge}(1-11)$  planes, lead to the observation of a  $\text{Ge}$  111 reflection in the pole figure, at  $\psi=39^\circ$  and  $\phi=0^\circ$ . This reflection is marked with a dotted red circle and labeled  $a^*(1-11)$  in Fig. 3(a). Similarly,  $a^*(11-1)$  and  $a^*(-111)$  correspond to the twinning of the  $\text{Ge}(111)$  surface plane relatively to the  $(11-1)$  and  $(-111)$   $\text{Ge}$  planes. The other secondary reflections located at  $\psi=56^\circ$  correspond to the twinning of the  $\text{Ge}(1-11)$ ,  $(11-1)$ , and  $(-111)$  inclined plane relatively to each other. Such twins have already been observed by Schroeder *et al.* during the growth of  $\text{Ge}$  on  $\text{Pr}_2\text{O}_3$ .<sup>10</sup> Their formation has been interpreted as occurring during the coalescence of the initially formed  $\text{Ge}$  islands, due to the presence of facets at the surface of these islands.

The  $\omega$ - $2\theta$  rocking curves recorded around the Ge 111,  $a11-1$ ,  $b11-1$ , and  $a^*1-11$  reflections of the pole figure of Fig. 3(a) are plotted in Fig. 4. The rocking curve recorded around the Ge 111 symmetric reflection presents two well resolved peaks centered at  $\omega=13.65^\circ$  (Ge 111 reflection) and  $\omega=14.25^\circ$  (Si 111 reflection). This confirms that the Ge layer presents the same (111) out of plane orientation as that of the Si substrate. The rocking curves recorded around the Ge  $a11-1$  reflection also present two peaks corresponding to  $a\text{Ge}$  111 and  $a\text{Si}$  111 reflections, respectively. This indicates that the in-plane orientation of the Ge variant  $a$  is the same as that of the Si substrate. The rocking curves recorded around the Ge  $b11-1$  (Ge variant  $b$ ) presents a significantly different shape: the intensity of the Ge 111 peak is 1700 times smaller than that of variant  $a$ . Since all the peaks correspond to reflections with the same 111 structure factor and with the same geometrical angle  $\psi$ , the diffracted intensities can be directly compared to quantify the proportion of the two variants. This indicates that 0.06% of the Ge layer is twisted  $60^\circ$  around the (111) vertical direction with respect to the Si substrate. The Si 111 reflection is not detected on this rocking curve, as expected for a single crystalline and single domain substrate. The peak centered at  $\omega=14.38^\circ$  is a 111 reflection of the  $\text{Gd}_2\text{O}_3$  layer. The  $\text{Gd}_2\text{O}_3$  lattice is rotated  $60^\circ$  around the (111) vertical direction with respect to the Si substrate, as already shown in Refs. 11, 13, and 14. In the end, the rocking curve recorded around the secondary  $a^*1-11$  Ge reflection at  $\psi=36^\circ$  and  $59^\circ$  only presents  $a\text{Ge}$  111 reflection, showing that only the Ge crystal is twinned with respect to the  $\{111\}$  asymmetric planes. Since the geometrical angles differ, the quantification of these secondary twinned variants is not possible. Nevertheless, the intensity in these rocking curves is several orders lower than the intensity of the rocking curves collected at  $\psi=70^\circ$  for the main variant  $a$ . This qualitatively indicates that only a few part of the Ge material is twinned with respect to the  $\{111\}$  asymmetric planes.

The results discussed in this section allow determining the relative orientations of the layers in the Ge/ $\text{Gd}_2\text{O}_3$ /Si heterostructure (Fig. 5). The epitaxial relationship between Ge,  $\text{Gd}_2\text{O}_3$ , and Si can be defined as  $[1-10]\text{Ge} (111) \parallel [-110]\text{Gd}_2\text{O}_3 (111) \parallel [1-10]\text{Si} (111)$ . Only 0.06% of the Ge material is twisted around the (111) vertical direction with respect to the main Ge variant, and a very few part of the Ge material is twinned with respect to the asymmetric (111) planes.

#### IV. CONCLUSION

In conclusion, we have demonstrated that crystalline  $\text{Gd}_2\text{O}_3/\text{Si}$  (111) templates could be used for the integration of Ge on silicon. Germanium grows in the Volmer–Weber

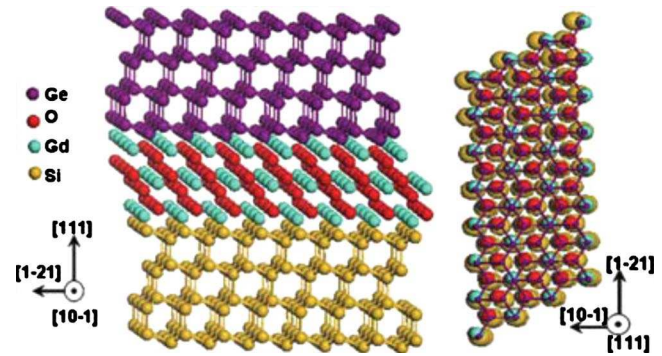


Fig. 5. (Color online) Schematics of the Ge/ $\text{Gd}_2\text{O}_3$ /Si stack, cross-section view (left) and top view (right).

mode and takes its lattice parameter as soon as growth begins, as already observed for several highly dissimilar semiconductor/oxide systems. 0.06% of the Ge material is twisted  $60^\circ$  around the vertical (111) direction, and a few part of the Ge material is twinned with respect to the  $\{111\}$  asymmetric planes. Future work will be focused on the clear identification of the origin of these twins and on the optimization of the Ge growth conditions in order to avoid their formation, thus to develop the quality of the Ge epitaxial film.

#### ACKNOWLEDGMENTS

This work is partly supported by the French Rhône-Alpes project “IMOX” and by the French ANR projects “BOTOX” (Project No. ANR05-JCJC-0055) and COMPHETI. The authors gratefully thank J. B. Goure and C. Bottela for technical assistance.

<sup>1</sup>R. People and J. C. Bean, Appl. Phys. Lett. **47**, 322 (1985).

<sup>2</sup>J. W. Seo *et al.*, Microelectron. Eng. **84**, 2328 (2007).

<sup>3</sup>A. Giussani *et al.*, J. Appl. Phys. **103**, 084110 (2008).

<sup>4</sup>G. Saint-Girons *et al.*, Appl. Phys. Lett. **92**, 241907 (2008).

<sup>5</sup>G. Saint-Girons *et al.*, Appl. Phys. Lett. **104**, 033509 (2008).

<sup>6</sup>J. Cheng, P. Regreny, L. Largeau, G. Patriarche, O. Mauguin, K. Naji, G. Hollinger, and G. Saint-Girons, J. Cryst. Growth **311**, 1042 (2009).

<sup>7</sup>G. Saint-Girons, P. Regreny, L. Largeau, G. Patriarche, and G. Hollinger, Appl. Phys. Lett. **91**, 241912 (2007).

<sup>8</sup>G. Saint-Girons, J. Cheng, P. Regreny, L. Largeau, G. Patriarche, and G. Hollinger, Phys. Rev. B **80**, 155308 (2009).

<sup>9</sup>T. Schroeder, P. Zaumseil, O. Seifarth, A. Giussani, H.-J. Müssig, P. Storck, D. Geiger, H. Lichte, and J. Dabrowski, New J. Phys. **10**, 113004 (2008).

<sup>10</sup>T. Schroeder, A. Giussani, H. J. Müssig, G. Weidner, I. Costina, Ch. Wenger, M. Lukosius, P. Storck, and P. Zaumseil, Microelectron. Eng. **86**, 1615 (2009).

<sup>11</sup>G. Niu, B. Vilquin, N. Baboux, C. Plossu, L. Becerra, G. Saint-Girons, and G. Hollinger, Microelectron. Eng. **86**, 1700 (2009).

<sup>12</sup>G. Profeta and E. Tosatti, Phys. Rev. Lett. **95**, 206801 (2005).

<sup>13</sup>T. Schroeder *et al.*, J. Appl. Phys. **102**, 034107 (2007).

<sup>14</sup>A. Fissel, D. Kühne, E. Bugiel, and H. J. Osten, Appl. Phys. Lett. **88**, 153105 (2006).